Asian Journal of Chemistry; Vol. 25, No. 17 (2013), 9537-9542

ASIAN JOURNAL OF CHEMISTRY

http://dx.doi.org/10.14233/ajchem.2013.15064

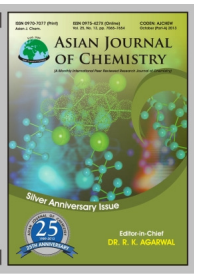

DFT Study of Xenon Complexes Adsorption on Graphene and Metal Embedded Graphene

BIN HUANG*, DINGZHONG YUAN and BIBO CHEN

Department of Materials Science and Engineering East China Institute of Technology, Fuzhou 344000, P.R. China

*Corresponding author: Tel/Fax: +86 794 8258320; E-mail: bhuang@ecit.cn

(*Received*: 31 December 2012; *Accepted*: 1 October 2013) AJC-14223

In this paper, periodic density functional theory calculations have been performed to study the adsorption of xenon complexes on intrinsic, Pt-doped and Cu-doped graphene sheets, respectively. Compared with the intrinsic graphene, metal doped graphene can strongly adsorb xenon atom and xenon complexes with higher binding energy value and shorter distance between the xenon atom and the graphene surface. Furthermore, we also demonstrate that the adsorption of XeF and XeBeO on metal doped graphene sheet are dissociation adsorption modes due to their high dipole moment. The density of states (DOS) results and the electronic density difference image indicate that the xenon complexes were strongly adsorbed on metal doped graphene by orbital hybridization, but no evidences for the hybridization between xenon complexes and intrinsic graphene sheet. We believe our calculations are useful to understand available experimental results.

Key Words: DFT, Xenon complexes, Graphene, Metal doped graphene, Density of states.

INTRODUCTION

Rare-gases and their compounds attract research interests for their notable inertness and their nearly continuous spectrum. Wiliam Ramsay observed the presence of rare-gases, since then, especially in recent years, exploration of rare-gases have attracted considerable attention in the laboratory[1]. The noble gas compounds that have been formed and in most of them, xenon atom bonds to highly electronegative atoms such as fluorine or oxygen, which is of HN_gY form (N_g is inert atoms and Y is electronegative atoms or groups). Except for HN_gY form, ArBeO, KrBeO and XeBeO molecules have also been detected in experiments and investigated by theoretical methods[2-4].

It is well known that accurate knowledge of the binding sites and orientation of molecules adsorbed on surfaces is an important component of surface science. The adsorption of xenon on graphite or close-packed transition-metal surfaces have been extensively investigated in recent years[5-8]. Several scanning tunneling microscopy (STM) and low-energy electron diffraction (LEED) experiments were performed, respectively, for xenon on Pt(111)[9], Ru(0001)[10] and Cu(111)[11]. These experiments found that the xenon preferentially attached to the low-coordinated on-top site instead of the high-coordinated hollow site on the metal surface. Density functional theory (DFT) calculations have also been successively carried out for xenon on close packed metal surfaces, such as Pt(111), Pd(111), Cu(111), Cu(110) and Ag(001), the calculation results also demonstrate that xenon preferentially occupies the on-top site on the metal surface[12-14]. In contrast to study on xenon adsorption on metal surface, the study of xenon adsorption on graphene is sparse in recent years[15]. The experimental analysis by a dynamical LEED shows that the hollow site preference for xenon on graphite and the equilibrium distance from xenon to graphene surface is 3.59 ± 0.05 Å. Only a few xenon adsorption on graphene systems have been theoretically studied, these calculations are typically based on *ab initio* and DFT calculations[16,17]. Especially, Sheng *et al.*[16] have elucidated the hollow site preference for xenon adsorption on graphene by MP2 method.

Graphene, a single atomic layer of graphite with surface only, can maximize the interaction between the surface dopants and adsorbates. However, theoretical studies show that NH_3, CO, H_2O, NO and NO_2 molecules are physically adsorbed on the intrinsic graphene[18,19]. Metal doped graphene can alter its electronic properties significantly, inducing a shift of the Fermi level and shallow acceptor states of the graphene, leading to its applicability extension[20]. In recent years, a number of theoretical studies were also performed to investigate the interactions between adatoms and graphene, which emphasize on the stable configurations of metal adatoms on graphene and charge transfer between metal adatoms and graphene. From these calculations, it is found that metal graphene is newly reported to make highly sensitive sensors, for example, the Al-doped graphene has high sensitivity to the CO molecules and HF molecules, respectively[21].

In the present contribution, we used density functional theory (DFT) calculations to investigate the nature and role of xenon complexes adsorption on both intrinsic graphene and Pt- or Cu-embedded graphene. The adsorption energies, the net electron transfers and the densities of state (DOS) of the systems were studied. Moreover, we also develop a discussion of the adsorption modes of intrinsic graphene and Pt- or Cu-doped graphene for xenon complexes.

COMPUTATIONAL METHOD

We carried out all-electron DFT calculations using double numerical basis sets with polarization function (the DNP basis set) implemented on the DMol3 package. Spin-unrestricted DFT in the generalized-gradient approximation(GGA) with the Perdew-Burke-Ernzerhof (PBE)[22,23] functional was used to obtain all the results given below. In order to take into account dispersion and corrections, xenon complexes adsorption on intrinsic graphene and metal doped graphene will be described as being at the PBE+D level. In the generation of the numerical basis sets, the global orbital cutoff is chosen to be 4.1 Å. The energy tolerance in the self-consistent field calculations is set to 10^{-6} E_h. Optimized geometries were obtained using an energy convergence tolerance of 10^{-5} E_h and a gradient convergence of 2×10^{-3} E_h $Å^{-1}$. The working cell is a 80-atoms $5 \times 4 \times 1$ supercell, with a vacuum of 18.00 Å along the z direction, which ensures that the z-axis of the periodic supercell is large enough so that there is no interaction between graphene sheets of adjacent supercells. The Brillouin zone was sampled using the Monkhorst-Pack special k-point scheme with a $5 \times 5 \times 1$ mesh for structural optimization and total energy calculations.

To evaluate the interaction between xenon complexes and adsorption sheet surface, we also calculated the adsorption energy (E_{ads}) of adsorbed systems, which is defined as

$$E_{ads} = E_{total} - (E_{sheet} + E_{adsorbate}) \quad (1)$$

where the E_{total}, E_{sheet} and $E_{adsrbate}$ denote the total energy of xenon complexes adsorption on intrinsic or metal doped graphene, intrinsic graphene or metal doped graphene and xenon complexes, respectively.

RESULTS AND DISCUSSION

Properties of metal doped graphene: The unique electronic property and geometric structure of doped graphene determine the activity and behaviour in the adsorption process. Platinum atoms in layers consisting of one or two graphene planes have been monitored at high temperature by high-resolution TEM[24]. Moreover, in the previous studies of the transition metal-atom-embedded graphene using density functional theory (DFT), it was found that the bonding between the transition-metal atom and neighboring carbon atoms manipulates the magnetic and electronic structures of the system. To simulate xenon complexes adsorption on doped graphene sheet, the Pt-doped and Cu-doped graphene system was made by replacement of the center carbon atom by a Pt and Cu atom (Fig. 1a), respectively. The calculated hexagon C–C bond length in graphene model is 1.42 Å, corresponding to the results reported previously. In contrast to intrinsic graphene,

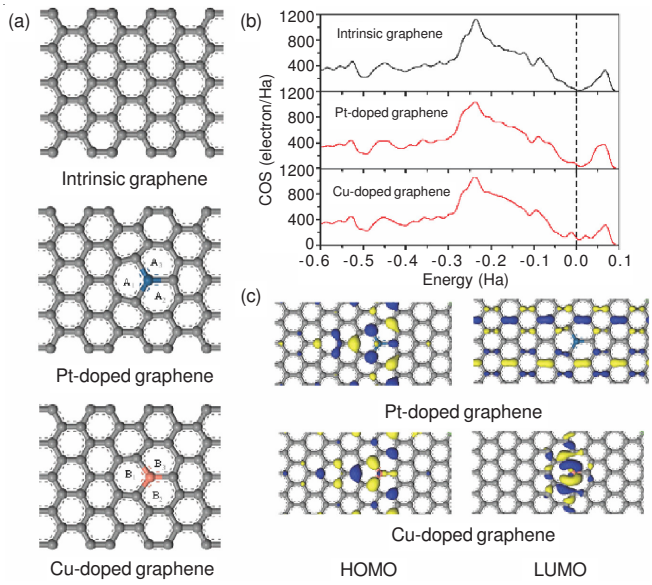

Fig. 1. (a) The optimized structure (b) Total density of states of the graphene sheet, Pt-doped graphene and Cu-doped graphene (c) The highest occupied molecular orbital (HOMO) and the lowest unoccupied molecular orbital (LUMO) of Pt-doped graphene and Cu-doped graphene at the Γ point

additional Pt and Cu atoms causes deformation of the nearby hexagonal rings in the doped region, but doped graphene remains planar structure, the Pt-C distances (A1, A2 and A3 in Fig. 1a) between Pt and carbon atoms are all 1.831 Å, respectively and the Cu-C distances (B1, B2 and B3 in Fig. 1a) between Cu and carbon atoms are all 1.717 Å, respectively.

Fig. 1c illustrates the isosurface of the highest occupied molecular orbital (HOMO) and the lowest unoccupied molecular orbital (LUMO) of two doped systems. It is well known the HOMO and LUMO of the graphene sheet are widely delocalized over the graphene surface, the HOMO and LUMO of the Pt-doped graphene are also widely delocalized over the graphene surface (Fig. 1c). However, in the case of LUMO in the Cu-doped graphene, the orbital is localized in the vicinity of Cu atoms. Xenon atom usually acts as the electron donor, this discrepancy of the LUMO of the Cu-doped graphene and the Pt-doped graphene may lead to the difference of xenon adsorption sites on the graphene. The total electron density of states (DOS) of the graphene, Pt- and Cu-doped graphene are shown in Fig. 1b, respectively. Obviously, more states are found for the Pt-doped graphene and the Cu-doped graphene lying round near the Fermi level compared to intrinsic graphene, so we propose the Pt-doped graphene and the Cu-doped graphene easily interact with xenon complexes than the intrinsic graphene.

Xenon adsorption on metal doped graphene: Firstly, we searched for the most stable configuration of xenon adorption on the intrinsic graphene, high-symmetry adsorption sites, top (T) site, two-fold bridge (B) and four-fold hollow (H) all are considered, respectively. The most stable structure of xenon adsorption on intrinsic graphene are shown in Fig. 2a. From our calculations, xenon preferentially bonds to the hollow site, which is more stable in energy (10.9 meV) than the on-top site and more stable (12.4 meV) than the bridge site, the calculated distance 3.652 Å from the surface to

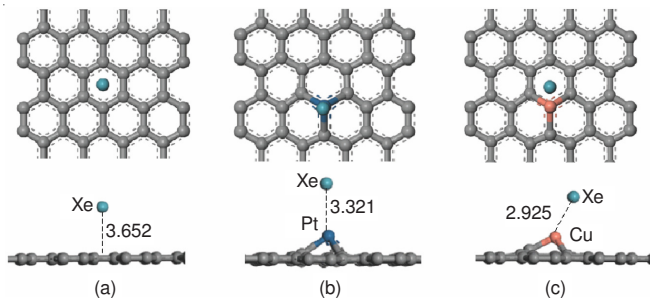

Fig. 2. Most stable configurations for xenon adsorption (a) intrinsic graphene, (b) Pt-doped graphene and (c) Cu-doped graphene.

the xenon atom is almost identical to the top and bridge adsorption, the calculated adsorption energy is -0.175 eV as shown in Table-1, indicating it is physisorption. The recent analysis[16] by the MP2 method had concluded that rare-gas xenon atom prefered to adsorb at the hollow site on graphite, the calculated adsorption energy is -0.134 eV and the equilibrium distance from xenon to the PAH model surface is 3.56 Å. In our calculation, we must be aware that such weak interactions are not well described by conventional DFT-GGA theory compared to MP2 calculations in xenon adsorption on graphene, in order to take into account dispersion and corrections, xenon complexes adsorption on intrinsic graphene will be described as being at the PBE + D level. However, in this paper, we also focus on xenon complexes adsorption on metal doped graphene and in previous studies, GGA-PBE functionals are capable of describing such systems, we also carried out GGA-PBE as the appropriate approach for studying the other systems.

TABLE-1
NET MULLIKEN ELECTRON POPULATION AND ADSORPTION ENERGY FOR XENON ADSORBED ON INTRINSIC GRAPHENE AND METAL DOPED GRAPHENE AT PBE+D LEVEL

	Net Mulliken charge |e|	E_{ads} (eV)
Intrinsic graphene	0.006	-0.175
Pt-doped graphene	0.107	-1.84
Cu-doped graphene	0.142	-2.47

The most stable structures of xenon adsorption on Pt-doped and Cu-doped graphene are shown in Fig. 2b and 2c, respectively. Compared with xenon adsorption on intrinsic graphene, xenon preferentially binds to the top site in the Pt-doped system and the approximate hollow sites in Cu-doped system, the distances from xenon to Pt and Cu atoms are 3.321 and 2.925 Å, respectively. In fact, the electronic character of the adsorbate and substrate can determine the adsorption site preference, so the difference site preference for xenon adsorption can be analyzed from the electronic structure of the substrate. In pristine graphene environment, the p_z orbitals of the carbon atoms contribute to the molecular π-type orbitals, because of these delocalized π electrons, graphene has donor-like character at the on-top region, while it has acceptor-like character at the hollow region. When the neutral xenon atom approaches the graphene surface, the Pauli repulsion force, naturally, drives the adatom to the hollow site, which tends to accommodate the valence electrons of xenon. For the xenon adsorption Pt-doped graphene, due to Pt-5*d* orbital playing an acceptor-like role, thus xenon binds to the on-top site on the Pt-doped surface. xenon adsorption Cu-doped graphene is different from Pt-doped system, xenon binds to the approximate hollow sites in Cu-doped systems, it may be caused by different d orbitals in Cu atoms. From Fig. 1c, we also can find LUMO mainly located in the C atoms for Pt-doped graphene and in the Cu atoms for Cu-doped graphene, so xenon weakly interacts with Pt atom in comparison with the interplay between xenon and Cu atoms.

The corresponding adsorption energies and charge transfer from the adsorbates to graphene are listed in Table-1. The adsorption energies of the xenon adsorption on intrinsic graphene are small and there is no evidence of formation of chemical adsorption. However, the adsorption energies on Pt- and Cu-doped graphene are -1.84 and -2.47 eV, respectively, which is more than the xenon adsorption on intrinsic graphene, indicating xenon atom interact strongly with Pt or Cu atoms. We further analyzed the electron distribution of the xenon adsorption on intrinsic graphene, Pt- and Cu-doped graphene, respectively. Table-1 shows that during the xenon adsorption on intrinsic graphene, 0.006 e transferred from the xenon atom to intrinsic graphene, 0.107e transferred from the xenon atom to the Pt-doped graphene and 0.142 e transferred from the xenon atom to the Cu-doped graphene, respectively, which is accordant with the adsorption energy. Fig. 6 shows the density of state for Pt-doped and Cu-doped graphene with xenon complexes adsorption. As shown in Fig. 6a, the density of state shows that the xenon hybridizes with Pt atom at -4.5 eV relative to the Femi level. Xenon highest occupied molecular orbital is -4.5 eV, which can be populated by the sheet electrons as a result of thermal excitations, so the overlap of orbitals would form a covalent bond between the xenon atom and the Pt-doped graphene. As a result, the covalent interactions between the xenon atom and the Pt-doped graphene contribute to the bonding of the adsorption. The density of state in Fig. 6b also shows that the xenon hybridizes with Cu atom and C atoms at -4.0 eV relative to the Femi level, but density of state of Cu atom span Fermi level, leading to interactions between the xenon atom and the Cu-doped graphene.

Xenon complexes adsorption on graphene: Five polar molecules XeF, XeBeO, FXeBO, FXeCCH, FXeCCN adsorption on graphene are investigated by DFT, the dipole moments are calculated as 2.96, 8.98, 1.22, 3.64 and 0.59 D for XeF, XeBeO, FXeBO, FXeCCH and FXeCCN as shown in Table-2, respectively. Fig. 3 plots xenon complexes adsorption on the graphene nanosheets, from our calculations, adsorption of five containing xenon molecules does not impact the structure of graphene distinctly. However, for XeBeO molecule, the electron-withdrawing ability of the BeO group is so strong that the charge is partially transferred from the π system of the graphene surface to the adsorbate (Fig. 3b), the strongly polarized XeBeO is natural to adsorb at the on-top site where aromatic π electrons is rich. However, as for four other molecules, the electron-withdrawing ability is moderate and the competition for electrons between molecules and the π system of graphene is not significant so that charge transfer is unremarkable, even at the on-top and bridge sites. Hence, there is no strong indication for the adsorption site preference for

TABLE-2
MULLIKEN ELECTRON POPULATION AND ADSORPTION ENERGY FOR DIFFERENT XENON COMPLEXES ON GRAPHENE AT PBE+D LEVEL

Molecule	Dipole moment	Net Mulliken charge |e|	E_{ads} (eV)
XeF	2.96	0.008	-0.138
XeBeO	8.98	0.023	-0.156
FXeBO	1.22	0.003	-0.119
FXeCCH	3.64	0.004	-0.121
FXeCCN	0.59	0.005	-0.115

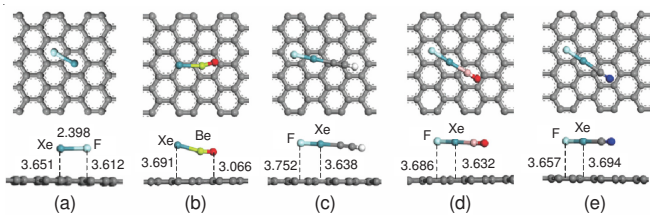

Fig. 3. Xenon complexes adsorption on graphene (a) XeF (b) XeBeO (c) FXeBO (d) FXeCCH (e) FXeCCN

for XeF, FXeBO, FXeCCH and FXeCCN molecules. The adsorption energy also prove the weak interaction between xenon complexes with graphene as shown in Table-2.

The net electron transfer is also calculated by Mulliken charge analysis as shown in Table-2. In the XeBeO adsorbed systems, 0.023e is transferred from the intrinsic graphene to XeBeO molecules, which is larger than other adsorbed systems. Overall, the charge transferred from the intrinsic graphene to the different molecules is relatively small in all systems, also indicating that the interaction between the xenon complexes and the intrinsic graphene sheet are mainly electrostatic in nature. Fig. 6c is the density of state of XeBeO-graphene system, comparing the density of state of XeBeO-graphene with that of intrinsic graphene, we can see that there is no hybridization between the XeBeO molecule and intrinsic graphene and the graphene states are nearly unaltered by the adsorption of the XeBeO molecule. Fig. 5a shows the electronic density differences images of XeF-graphene. No charge accumulation could be seen between the intrinsic graphene and the XeF molecule. All results indicate that the interaction between the xenon complexes and the intrinsic graphene is of weak vander Waals interaction type and the adsorption is by weak physisorption.

XeF and XeBeO adsorption on doped graphene: To find the most favorable adsorption configuration, 4 initial adsorption configurations were considered in XeF adsorption on Pt-doped graphene, which are distributed into two highly symmetric categories: XeF parallel to graphene surface and XeF perpendicular to graphene surface. The most stable relaxed structure of the initial adsorption configuration T-H is shown in Fig. 4a. Fig. 4a, we note that the distance between xenon atom and F atom is 3.637 Å in XeF adsorption on Pt-

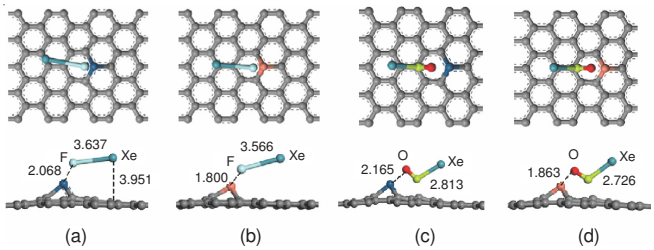

Fig. 4. XeF adsorption on (a) Pt-doped and (b)Cu-doped graphene and XeBeO adsorption on (c) Pt-doped and (d) Cu-doped graphene

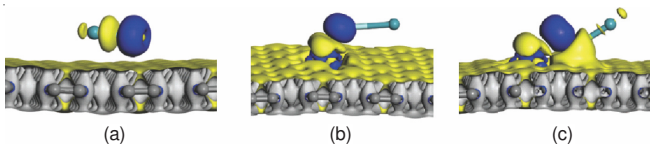

Fig. 5. Deformation charge density (a) XeF adsorption on graphene, (b) XeF adsorption on Pt-doped graphene and (c) XeBeO adsorption on Cu-doped graphene

doped graphene system, which is larger than XeF molecule adsorption on intrinsic graphene and the Pt-F distance is 2.068 Å, the results indicate XeF molecule occurred decomposition. Previous studies[25] have proved the interaction of metal and adsorbate will weaken the bonding in the adsorbed molecules, in our calculation, the formation of Pt-F bond also weaken the bonding of the adsorbed XeF molecules, which result in dissociation of XeF molecule on Pt-doped graphene surface. XeBeO molecule adsorption on metal doped graphene are also shown in Fig. 4, as shown in Fig. 4c, due to metal polarization, XeBeO also occur distortion, the Be-Xe distances becomes large, 2.813 Å larger 0.221 Å than XeBeO adsorption on intrinsic graphene. The similar phenomena are observed xenon complexes adsorption on Cu-doped graphene as shown in Fig. 4.

The calculated electron data and adsorption energy are shown in Table-3. Table-3 shows that the corresponding adsorption energy value of XeF and XeBeO molecules in the Pt-doped system are -6.43 and -4.51 eV, respectively, which is over 100 times more than that in intrinsic graphene. Due to XeF molecules decomposition, for comparsion, we also calculated the F atom adsorption on Pt doped graphene, the calculated adsorption energy is -6.23 eV, approximate the XeF adsorption on Pt-doped graphene. The electronic density difference image is shown in Fig. 5, the blue region indicates gained electrons, while the yellow region represents lost electrons. In Fig. 5b, there is charge accumulation between the F atom and the Pt-doped graphene and F atom of the XeF molecule gains electrons from the Pt-doped graphene, however, no charge accumulation happens on xenon atom, this demonstrates that the charge transfer would form an ionic bond between the F atom and the Pt-doped graphene. The above results are consistent with the data from Mulliken charge analysis as listed in Table-3, we found charge on xenon decrease from 0.129 to

TABLE-3
MULLIKEN ELECTRON POPULATION AND ADSORPTION ENERGY FOR XeF AND XeBeO ADSORPTION ON METAL DOPED GRAPHENE

	XeF			XeBeO		
	q (Xe)	q (F)	E_{ads} (eV)	q (Xe)	q (BeO)	E_{ads} (eV)
Pt-Doped graphene	0.003	-0.563	-6.43	0.015	-0.321	-4.51
Cu-Doped graphene	0.002	-0.530	-5.86	0.011	-0.283	-4.13

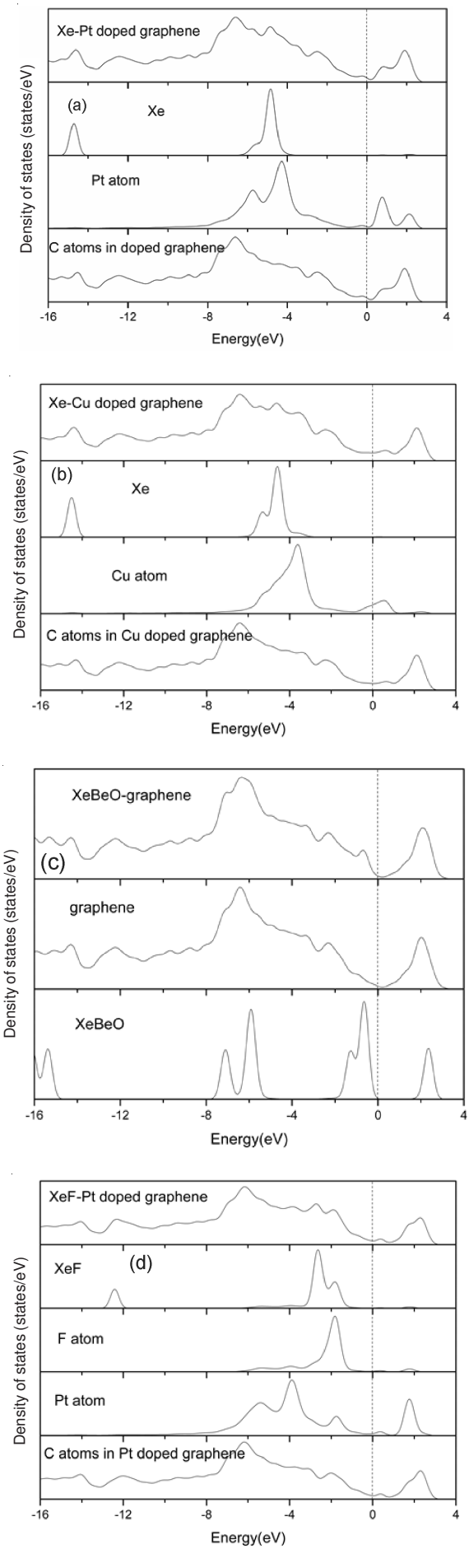

Fig. 6. Density of state (DOS) of (a) xenon adsorption on Pt-doped graphene, (b) xenon adsorption on Cu-doped graphene, (c) XeBeO adsorption on intrinsic graphene, (d) XeF adsorption on Pt doped graphene, (e) XeBeO adsorption on Pt doped graphene. Dash line represent E_f energy level

0.003e, 0.56 e is transferred from the Pt-doped graphene to the F atom, the result verifies the electronic transport properties of the pristine graphene are changed by the doping of Pt atom again. The density of state plot for the XeF-Pt-doped graphene system is determined and shown in Fig. 6d. Unlike the intrinsic adsorbed system, the adsorption of the XeF molecule alters the Pt-doped graphene electronic structure. The density of state results in Fig. 6d shows that the F atom hybridizes with Pt atom at -2.0 eV relative to E_f, therefore, both ionic bonds induced by the charge transfer due to the overlap of orbitals between F atom and Pt atom contribute to F adsorption on Pt doped graphene, but due to high dipole moment of XeF molecule, resulted in more larger distance between xenon atom and F atom.

Conclusion

In the present study, the adsorption of xenon complexes on graphene surfaces was investigated by first-principles theory. The adsorption configurations and electronic structure for intrinsic and metal doped graphene systems were established and analyzed the factors which affect on the adsorption process. Compared with the intrinsic graphene, metal doped graphene can strongly adsorb xenon atom and xenon complexes with higher binding energy value and shorter distance between the xenon atom and the graphene surface. Furthermore, we also demonstrate XeF and XeBeO adsorption on metal doped graphene sheet are dissociation adsorption modes due to their high dipole moment. The results of density of states results and the electronic density difference image indicate that the xenon complexes were strongly adsorbed on metal doped graphene by orbital hybridization, but no evidences for the hybridization between xenon complexes and intrinsic graphene sheet. Present results provide a basis for further experimental and theoretical exploration of containing inert atoms adsorption doped graphene surface.

ACKNOWLEDGEMENTS

This work was supported by Nature Science Foundation of Jiangxi Province (20114BAB213010) and the Foundation of Jiangxi Educational Committee (No. GJJ11487).

REFERENCES

1. N.N. Greenwood and A. Earnshaw, In Chemistry of the Elements; Butterworth-Heinemann: Oxford, 888 (2001).
2. L. Sheng, A. Cohen and B.R. Gerber, *J. Am. Chem. Soc.*, **128**, 7156 (2006).
3. G. Frenking, W. Koch, J. Gauss and D. Cremer, *J. Am. Chem. Soc.*, **110**, 8007 (1988).
4. C.A. Thompson and L. Andrews, *J. Am. Chem. Soc.*, **116**, 423(1994).
5. W.E. Carlos and M.W. Cole, *Surf. Sci.*, **91**, 339 (1980).
6. J.R Cerda, P.L. De andres, F. Flores and R. Perez, *Phys. Rev. B*, **45**, 8721 (1992).
7. P.A. Rejto and H.C. Andersen, *J. Chem. Phys.*, **98**, 7636 (1993).
8. M. Otthoff, G. Hilgers, N. Muller, U. Heinzmann, L. Haunert, J. Braun and G. Borstel, *Surf. Sci.,* **322**, 193 (1995).
9. T. Seyller, M. Caragiu, R.D. Diehl, P. Kaukasoina and M. Lindroos, *Phys. Rev. B*, **60**, 11084 (1999).
10. B. Narloch and D. Menzel, *Surf. Sci*., **412**, 562 (1998).
11. T. Seyller, M. Caragiu, R.D. Diehl, P. Kaukasoina and M. Lindroos, *Chem. Phys. Lett.*, **291**, 567 (1998).
12. J.L.F. Dasilva, C. Stampfl and M. Scheffler, *Phys. Rev. B*, **72**, 075424 (2005).
13. P.S. Bagus, V. Staemmler and C. Woll, *Phys. Rev. Lett.*, **89**, 096104 (2002).
14. M. Caragiu, T. Seyller and R.D. Diehl, *Surf. Sci.*, **539**, 165 (2003).
15. K. Pussi, J. Smerdon, N. Ferralis, M. Lindroos, R. MacGrath and R.D. Diehl, *Surf. Sci.*, **548**, 157 (2004).
16. S. Li, O. Yuriko and T. Tetsuya, *J. Phys. Chem. C*, **114**, 3544 (2010).
17. J.L.F. Dasilva and C. Stampfl, *Phys. Rev. B*, **76**, 085301 (2007).
18. O. Leenaerts, B. Partoens and F.M. Peeters, *Phys. Rev. B*, **77**, 125416 (2008).
19. B. Huang, Z.Y. Li, Z.R. Liu, G. Zhou, S.G. Hao, J. Wu, B.L. Gu and W.H. Duan, *J. Phys. Chem. C*, **112**, 13442 (2008).
20. Y. Qian, S.B. Lu and F.L. Gao, *Mater. Lett.*, **65**, 56 (2011).
21. C. Mei and Y.P. Zhao, *Comp. Mater. Sci.*, **46**, 1085 (2009).
22. J.P. Perdew, K. Burke and M. Ernzerhof, *Phys. Rev. Lett.*, **77**, 3865 (1996).
23. B. Delley, *J. Chem. Phys.*, **92**, 508 (1990).
24. Y. Qian and C.Y. Wang, *Appl. Surf. Sci.*, **257**, 10758 (2011).
25. A. Sumer and A.E. Aksoylu, *J. Phys. Chem. C*, **113**, 14329 (2009).